J Neurophysiol 107: 1291–1300, 2012.
First published November 30, 2011; doi:10.1152/jn.00177.2011.

Physical model of coherent potentials measured with different electrode recording site sizes

Matthew J. Nelson[1,2] and Pierre Pouget[1]

[1]*Centre de Recherche de l'Institut Cerveau-Moelle/Institut National de la Santé et de la Recherche Médicale, Unité Mixte de Recherche S975 du Centre National de la Recherche Scientifique 7225, Université Pierre et Marie Curie, Hôpital de la Salpêtrière, Paris, France; and* [2]*California Institute of Technology, Pasadena, California*

Submitted 1 March 2011; accepted in final form 24 November 2011

Nelson MJ, Pouget P. Physical model of coherent potentials measured with different electrode recording site sizes. *J Neurophysiol* 107: 1291–1300, 2012. First published November 30, 2011; doi:10.1152/jn.00177.2011.—A question that still complicates interpretation of local field potentials (LFPs) is how electrode properties like impedance, size, and shape affect recorded LFPs. In addition, how any such effects should be considered when comparing LFP, electroencephalogram (EEG), or electrocorticogram (ECoG) data has not been clearly described. A generally accepted concrete physical model describes that an electrode records the spatial average of the voltage across its uninsulated tip, yet the effects of this spatial averaging on recorded coherence have never been modeled. Using simulations based on this physical model, we show here that for any effects to occur, a spatial voltage gradient on a scale smaller than an electrode's recording site must exist over the site's surface. When this occurs, larger electrodes on average report higher coherence between locations, with the effect continuously increasing as the voltage profile over the extent of the recording site is increasingly nonuniform. We quantitatively compared published coherence estimates of LFP, ECoG, and EEG data across a range of studies and found a possible modest effect of electrode size in published ECoG data only. We used the model to quantify the expected coherence for any electrode size in relation to any given spatial frequency of a voltage profile. From this and existing estimates of the spread of voltages underlying each of these data types, our simulations quantitatively agree with the published data and importantly suggest that LFP coherence will be independent of recording site size within the range of microelectrodes typically used for extracellular recordings.

local field potentials; electrocorticogram; electroencephalogram; impedance

FOR MANY YEARS, local field potentials (LFPs) have proven to be an important data source for improving our understanding of the brain. Despite this, questions surrounding their interpretation still remain unanswered, but they have been a recent topic of renewed interest in the literature (Bedard et al. 2010; Katzner et al. 2009; Logothetis et al. 2007; Xing et al. 2009).

One such question that often arises is: what effect do properties like electrode impedance and shape have on recorded LFPs? We argued previously (Nelson and Pouget 2010) that when interpreting LFP recordings from microelectrodes, neurophysiologists can ignore for all practical purposes the particular size and shape of recording sites provided that they are within the ranges normally used for extracellular recordings. The basis for this argument originates from a physical model of microelectrode recording circuits (Robinson 1968) that we confirmed experimentally in our previous work (Nelson et al. 2008). There we explicitly showed that with the use of an amplifier of appropriately high input impedance, which is available in some but not all commercially available recording equipment, the impact on recorded signals of the electrical impedance of the microelectrode/tissue interface is negligible. The voltage recorded by a microelectrode in this case will equal the average voltage present across its uninsulated tip. Yet, recording site size could still potentially influence recordings on a physical basis by affecting what that average voltage at the electrode's tip is. This could occur if the underlying voltage being measured varies spatially on a scale finer than an electrode's recording site size. However, current estimates of the spatial extent of the LFP suggest that 95% of the signals recorded at a given point in space originate from within a 250-μm radius (Katzner et al. 2009), which well exceeds the size of microelectrode recording sites for the ranges of microelectrodes typically used by neurophysiologists (Lemon 1984; Tielen et al. 1971; Yaeli et al. 2009). Thus the particular size of these recording sites should not affect the LFP signals they record.

Claims that electrode size and shape should affect recorded LFPs have been made in the literature (e.g., Berens et al. 2008; Kay and Lazarra 2010; Pesaran 2009) without mention or apparent consideration of this generally accepted theoretical basis of the nature of microelectrode recordings (Robinson 1968). Many neurophysiologists do have some familiarity with a notion that larger electrodes record signals from more distant sources and that this results in differences between the signals recorded by electrodes of different sizes. However, the separation of the discussion in the literature from the basic physical nature of the recordings may obscure to many in the field the fact that electrodes average only the signals that exist over the spatial extent of their recording site surface areas. Surprisingly, although electrode size has been modeled in different aspects before (e.g., Lempka et al. 2011; Moffitt and McIntyre 2005; Ollikainen et al. 2000), models of how this simple spatial averaging directly affects recorded signals have not appeared in the literature to our knowledge. This is the case despite the existence of strong claims that, for example, this spatial averaging property should cause different microelectrode sizes within the brain to reveal fundamentally different voltage signals (Nunez and Srinivasan 2006).

There have been some empirical investigations of the effect of electrode size on the coherence of recorded LFPs, with unclear results. Bullock and McClune (1989) reported finding

Address for reprint requests and other correspondence: M. Nelson, CRICM, UMR S975, INSERM/Université Pierre et Marie Curie, Neurologie et Thérapeutique Expérimentale, Hôpital de la Salpêtrière, 47 boulevard de l'Hôpital, 75651 Paris Cedex 13, France (e-mail: matthew.nelson@upmc.fr).

no difference in coherence when comparing electrode recording sites with 1-μm diameters to those with 50-μm diameters or when comparing those with 25-μm diameters to those with 250-μm diameters. Kay and Lazzara (2010) later compared coherence between electrodes of very different sizes (200- vs. 2- to 3-μm diameters). They found that the much larger electrodes reported slightly more coherence, although the spectral power was the same between the different electrode sizes. Despite the very large difference in the size of the electrodes they compared, the effects that they reported were very small, and thus their results are not per se incompatible with our earlier claim. Still, if these effects do hold true for large electrode differences, it raises a question as to whether this should be considered when comparing LFPs to electroencephalogram (EEG) data recorded from the scalp or electrocorticogram (ECoG) data recorded from the cortical surface, both of which are typically done with much larger electrodes.

In addition to the empirical ambiguity surrounding the question, the theoretical prediction of how averaging signals across larger regions of space should be expected to affect the coherence of recorded signals is unclear a priori. Competing effects are present; some effects would cause larger electrodes to tend to report more coherence, whereas some effects would cause smaller electrodes to tend to report more coherence. Thus we sought to test what the expected overall effect is through quantitative simulations based on the theoretical basis of microelectrode recordings.

In this report we explicitly describe a simple physical model to clearly illustrate the theoretical basis through which claims about the effect of electrode size and shape on recorded potentials should be considered. Importantly, this model highlights that for any differences between recording sites to occur, the underlying voltage profile must vary appreciably over the extent of the larger recording site's surface. We then use quantitative simulations of the model using simulated and real LFP traces to test the nonobvious result of whether larger electrodes should report higher levels of coherence. We found that the modeled low-impedance electrodes do indeed report larger coherences between areas than the modeled high-impedance electrodes. We show that this effect continuously increases as the voltage profile is increasingly nonuniform over the extent of the larger electrode's recording site and that it is robust with respect to the strength of the coherence gradient along the voltage profile. We then quantitatively compare coherence reported in LFP, ECoG, and EEG data across several studies and laboratory groups and find evidence for a possible modest effect of electrode size in ECoG data only. We extend our simulations to quantify the effect on recorded coherence of any given ratio of electrode size to the spatial frequency of the underlying neural activity. Combining this with published estimates of the spatial frequencies present in each neurophysiological data type confirms the trends we observed in the literature.

MATERIALS AND METHODS

The model. It is trivial to conclude but bears mentioning a priori that the LFP signal must vary appreciably over the size of the lower impedance electrode tip for the electrode impedance to have the possibility to make any difference at all in the resulting recorded value (Nelson and Pouget 2010). This point should be further obvious if one considers the extreme opposite case in which the LFP signal is spatially uniform. It is clear that in this case, the particular locations over which the voltage is averaged by electrodes of different sizes would not matter.

Figure 1*A* shows the most basic version of a physical model of how differences in coherence could be observed between electrodes of different sizes. In this model, some subregions are highly coherent between two distant locations, whereas some are not. Potentials recorded in the subregions with high distant coherence are highly coherent with each other, whereas potentials in the subregions with low distant coherence are not coherent with either subregion. Very low impedance electrodes that are large relative to the size of the subregions would extend across the subregions (Fig. 1*B*, *left*) and would thus always report the average activity between the subregions. In contrast, microelectrodes that are small relative to the size of the subregions would tend to fall into a single subregion and would thus reflect the activity of one or the other subregion by chance depending on the random precise placement of the electrode (Fig. 1*B*, *right*). In this situation, the low-impedance electrodes would reliably have moderate coherence, because the voltage they record would always include that of the high distant coherence subregion, but this activity would also always be averaged with that of the less coherent low distant coherence subregion. In contrast, the microelectrodes would occasionally record very low coherence on some recordings when they happen to be in low distant coherence subregions, but they would also occasionally record very high coherences when both electrodes happened to be in high coherence subregions. Competing effects would thus be present in determining which electrode type would be

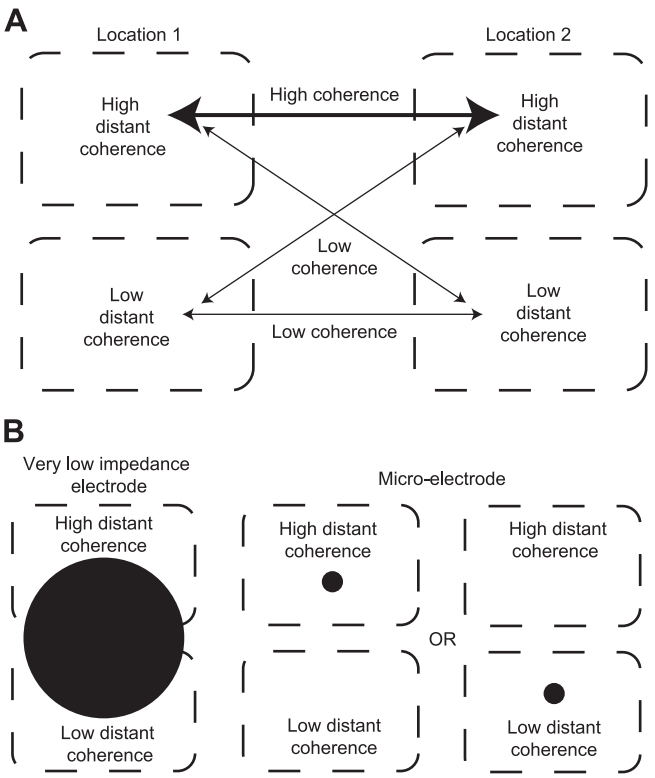

Fig. 1. Simple model of a local field potential (LFP) activity profile to produce a difference in recorded coherence between electrode types. *A*: diagram of discrete subregions in 2 distant locations with different patterns of coherent activity. The subregions between the locations with high distant coherence are highly coherent with each other, whereas those subregions with low distant coherence are neither coherent with each other nor coherent with the high distant coherence subregions. *B*: basic model of different electrode types within the 2 locations. Very low impedance electrodes span both subregion types and are modeled to average the activity between them for each session. Microelectrodes are located in only 1 subregion at a time and are modeled to report the activity of a single randomly selected subregion for each session.

expected to have the higher coherence on average, with the result depending on the properties of signal averaging before calculating coherence.

The basic model described above can be extended to make quantitative predictions for the expected effects of electrodes of particular sizes relative to the spatial variation of underlying neural activity. This can be done in the most general sense by modeling the underlying voltage profile as a spatial sine wave (see Fig. 6*A*), since any spatial variation of voltage can be described by the contributions of sine wave components at different spatial frequencies. In this version of the model, the voltage varies continuously by oscillating sinusoidally between high and low distant coherence activity instead of having each type of activity separately confined to distinct subregions as in the basic model. Electrode recording sites are modeled to be of precise sizes in relation to the spatial wavelength of the sinusoidal voltage profile and placed at random phases of the voltage profile, averaging the activity present along their lengths. Using these results, the effects for any particular voltage profile and electrode size could then be predicted.

Simulating high and low distant coherent activity. To produce testable data that captures the key points of the above models, we created four LFP traces. Each of the two simulated electrode locations in the basic model was composed of two traces: one corresponding to a high distant coherence subregion and one corresponding to a low distant coherence subregion. We did this with both purely simulated data and real LFP traces, following procedures described below. The goal in creating and selecting these traces for the primary simulations was to obtain two LFP traces that were highly coherent with each other, which represent the high distant coherence subregions in each location, and two LFP traces that were neither coherent with each other nor coherent with the previous traces, which represent the low distant coherence subregions in each location (see Fig. 1*A*).

Using simulated data. We generated simulated LFP signals in Matlab (The MathWorks, Natick, MA) by adding white noise to sinusoids with a simulated sampling rate of 1 kHz. The period of the sinusoid was set to 50.234 samples per cycle to avoid the unrealistic situation where this was exactly a multiple of the sampling period. This resulted in a signal frequency of just under 20 Hz. Two hundred trials of 4 s each were simulated for each session. The amplitudes and phases of the four signals across trials were determined by sampling from a multivariate normal distribution using the "mvnrnd" function in Matlab. For the primary simulations, we set the correlation coefficient for both amplitudes and phases to 0.8 between the pair of high distant coherence signals and 0.2 between all other signal pairs. For all signals, the mean amplitude was set to 10 arbitrary units with a variance of 2, and the arbitrary mean phase was set to 180 deg with a standard deviation of 60 deg. The standard deviation of the independent white noise added to the sinusoids was set to 1 for the two high distant coherence traces and 3 for the low distant coherence traces.

We performed two additional sets of simulations to investigate the effects when the coherence differences between the individual traces are smaller. To generate traces with a moderate coherence difference, we set the amplitude and phase correlation coefficients to 0.65 between the high coherence traces and 0.35 between all other traces. To generate traces with no coherence differences between them, we set the amplitude and phase correlation coefficients to 0.5 between all traces and set the standard deviation of the independent white noise added to all traces to 1. All other parameters were identical parameters to those described above for the primary simulations.

For the primary simulations, Fig. 2*A*, *left*, shows the four traces used from one sample trial using simulated data. The low coherence pair shows more white noise and uncorrelated deviation in their phases and amplitudes than the high coherence pair. Figure 2*B*, *left*, shows for one sample session the coherence of the four possible trace pairings between locations. This shows that the desired coherence pattern of a high coherence between the two high distant coherence traces but a low coherence between all other pairings of traces was indeed achieved. For one of the additional simulations to generate traces with no coherence differences between pairings, Fig. 4*A*, *left*, shows for one sample session the coherence of the four possible trace pairings between locations. This shows that the desired coherence pattern for this simulation of an equally moderate coherence between all pairings of traces across locations was again achieved, with some small random differences occurring each session by chance.

We also tested two other methods of simulating LFP traces with the desired coherence patterns. For one method, the signal amplitudes were determined as described previously, but the relative phases of trace pairs rather than the absolute phases of each trace were determined according to independent normal distributions. In this method, the relative phase between the traces of the higher coherence pair was selected to have a lower standard deviation than the relative phase between the traces of the lower coherence pair. In another method, both pairs were generated with the same phase distribution, but much more white noise was added to the lower coherence pair (100 arbitrary units), which served to sufficiently reduce the coherence involving those signals. Both of these alternative simulation methods yielded identical conclusions to the data we present here, so we decided to omit the results using these methods for presentation clarity and simplicity.

Using real data. Data were collected from one adult monkey (*Macaca mulatta*). The animal was cared for in accordance with policies set forth by the United States Department of Agriculture and Public Health Service Policies on the Humane Care and Use of Laboratory Animals. Animal care, procedures, and experiments were also carried out with the supervision and approval of the Vanderbilt Institutional Animal Care and Use Committee. Two recording chambers (RC-1; Gray Matter Research, Bozeman, MT) were surgically implanted into the animal's skull, targeting the frontal eye fields in each area. An eight-channel acute microdrive system (AC8-1; Gray Matter Research) was placed in each chamber. Recordings were subsequently made with glass-insulated tungsten microelectrodes (1–2 MΩ; Alpha Omega Engineering, Nazareth, Israel) from 1 to 2 mm below the depth at which spiking activity was first observed on each electrode. LFPs were measured relative to an externally grounded reference that was connected to the chamber and the microdrive casing. Voltage signals were amplified (×1) by a high-impedance HST/8050-G1 head stage (Plexon, Dallas, TX), filtered from 0.2 to 300 Hz using a custom-built analog filter (Plexon), further amplified (×1,000), and then digitally sampled at 1 kHz using a Plexon MAP system. The transfer function of the entire recording system was estimated and adjusted for using procedures described previously (Nelson et al. 2008). We performed a deconvolution using an inverse filter restricted to the bandwidth spanning from 0.5 to 450 Hz. Data from frequencies outside this range were attenuated too strongly to recover a stable estimate.

Neural data were recorded while the monkey performed a search-step task, similar to that reported in Murthy et al. (2001). Analyses were performed on data within a time window spanning from 50 to 650 ms following the target presentation, during which the recorded LFPs exhibited 20-Hz activity. Three hundred forty-two correct trials across all target locations were used. Four of 15 simultaneously recorded LFP traces were selected from a single recording session. The traces were selected manually on inspection of coherence between the channels. For the primary simulations, the traces were selected such that the coherence was high between one pair (designated to be the high distant coherence traces) and moderate to low between all other pairs. For an additional simulation performed to investigate the effects when coherence differences between the individual traces were smaller, a separate group of four traces was selected such that the coherence between all trace pairings was approximately equally moderate.

For the primary simulations, Fig. 2*A*, *right*, shows the four traces from one sample trial using real LFP data. Figure 2*B*, *right*, shows for

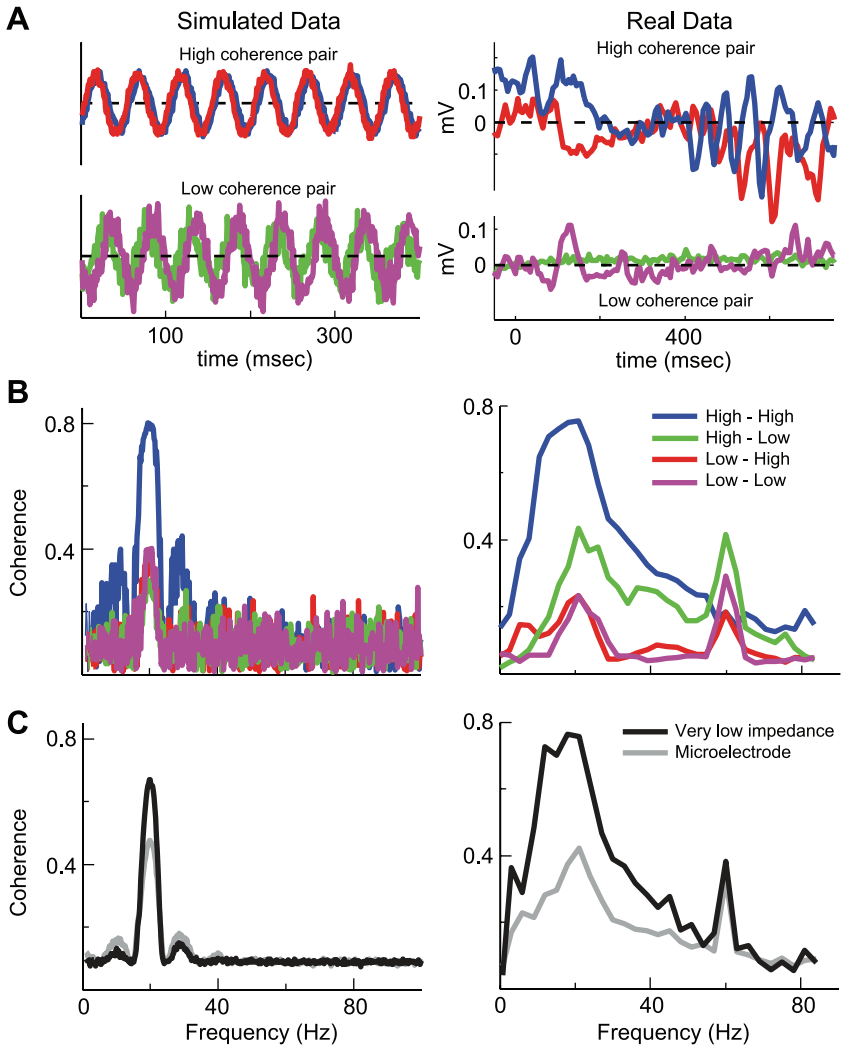

Fig. 2. Simulated coherence patterns using simulated and real LFP traces. *Left* panels correspond to results using simulated LFP traces, and *right* panels correspond to results using real LFP traces. *A*: sample individual signals for the signals with high distant coherence (red and blue) and the signals with low distant coherence (green and magenta). *B*: direct intersubregion coherence across 2 locations as labeled for the 4 subregion combinations. The high-high (blue) trace shows the direct coherence between the high distant coherence subregions in each location (see Fig. 1*A*); the high-low (green) trace shows the direct coherence between the high distant coherence subregion in *location 1* and the low distant coherence subregion in *location 2*; the low-high (red) trace shows the direct coherence between the low distant coherence subregion in *location 1* and the high distant coherence subregion in *location 2*; and the low-low (magenta) trace shows the direct coherence between the low distant coherence subregions in each location. *C*: average coherence across 500 sessions for simulated very low impedance electrodes (black lines) and simulated microelectrodes (gray lines). The high distant coherence fraction was set to the default value of 0.5.

one sample session the coherence of the four possible trace pairings between locations after assigning each trace to a location. Again, the desired coherence pattern was achieved in which the coherence was high between the two high distant coherence traces but low between all other pairings of traces. For the additional simulation using traces with approximately equally moderate coherence between all trace pairings, Fig. 4*A*, *right*, shows for one sample simulated session the coherence of the four possible trace pairings between locations. Again, the desired coherence pattern for this simulation of an approximately equally moderate coherence between all pairings of traces across locations was achieved.

Simulating electrode recordings: basic model. Using the four LFP traces generated from simulated or real data, for 500 simulated sessions we calculated the coherence between the locations for two simulated very low impedance electrodes and two simulated microelectrodes. To simulate the very low impedance electrodes, we calculated a weighted average of the activity of the high and low distant coherence traces for each location for each session (Fig. 1*B*, *left*). To simulate the microelectrodes, the voltage for each electrode was independently randomly selected to be either the high or low distant coherence trace for each session (Fig. 1*B*, *right*). To simulate different proportions of subregion space having high or low distant coherence, we adjusted what we refer to as the high distant coherent fraction. For the very low impedance electrodes, this fraction determined the relative weights of the high and low distant coherence traces when calculating the average between them. For microelectrodes, this fraction determined the probability that a high or low distant coherence trace would be selected each session. Simulations were run with this parameter set to 0.1, 0.25, 0.50, 0.75, and 0.9. Note that when real data were used, the individual traces themselves were the same between each session. Thus the same precise values were used for the simulated very low impedance electrodes for every session, although the simulated microelectrode coherence values using the real data changed randomly between sessions.

Simulating electrode recordings: spatial sine wave model. Using four simulated LFP traces, for 500 simulated sessions we calculated the coherence between locations for electrodes with different recording site lengths while the underlying voltage profile varied continuously between the high and low distant coherence traces for each location along a spatial sine wave. At the peak of the sine wave, the voltage was set to the high distant coherence activity for that location; at the trough of the sine wave, the voltage was set to the low distant coherence activity for that location; and in between, the voltage was set to a continuously varying weighted average of the two. For example, at the midway point of the sine wave, the voltage was the exact average of the two traces. Thus this weighted average precisely corresponds to the high distant coherence fraction of the basic model described above. The individual traces were generated using the same parameters as the primary simulations of the basic model, which were the parameters used to generate the results shown in Figs. 2 and 3. Electrode recording sites of different sizes were then modeled by averaging across different lengths of the sinusoid while randomly determining the phase each session according to a uniform distribution spanning from 0 to 360 deg. Recording site lengths were specified

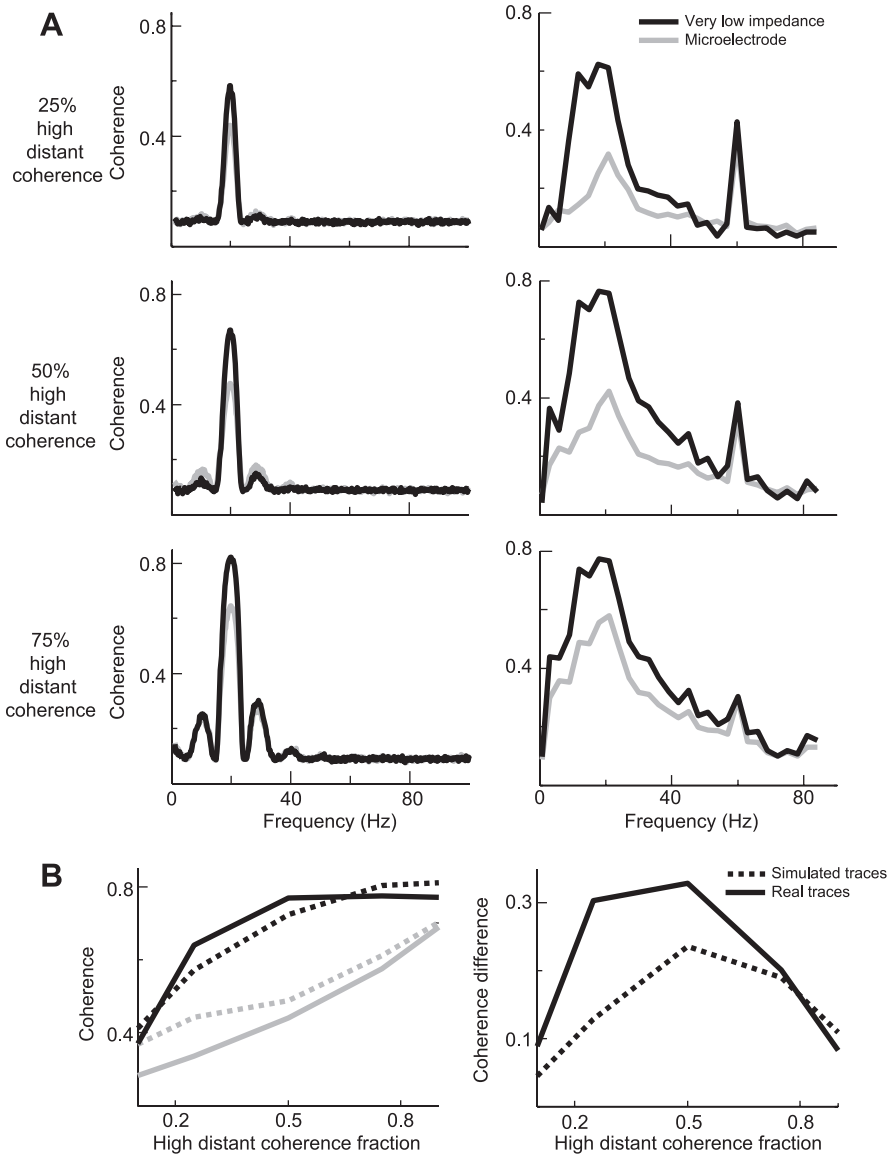

Fig. 3. Simulated coherence patterns of the basic model while varying the high distant coherence fraction. *A*: average coherence across 500 sessions for simulated very low impedance electrodes and simulated microelectrodes while setting the high distant coherence fraction to 0.25 (*top* row), 0.5 (*middle* row), and 0.75 (*bottom* row). *Left* panel corresponds to results using simulated LFP traces, and *right* panel corresponds to results using real LFP traces. *B*: average 20-Hz coherence while varying the high distant coherence fraction. *Left* panel shows the very low impedance electrode (black) and microelectrode (gray) average 20-Hz coherence across 500 simulated sessions using simulated (dashed) and real (solid) LFP traces at different values of the high distant coherence fraction. *Right* panel shows for the same data the difference between the simulated very low impedance electrodes and microelectrodes.

in units of the number of wavelengths of the underlying spatial sinusoid to allow for the generalization of the results to any voltage profile spatial frequency. The average activity along the recording site length was determined analytically through integration of the sinusoid.

Measuring coherence. We calculated the coherence across locations for each simulated session and electrode type and report for all simulations the average coherence across sessions. We calculated the coherence using techniques described in Jarvis and Mitra (2001). For the simulated data, we used one large window with a length equal to that of the entire 4 s of the simulated trial. For the real data, we used a 200-ms window sliding in time across a trial with a 10-ms step size. We then report the average coherence across time windows for the period of the trial used for the analysis, with the center of the window spanning from 150 to 550 ms after the initial appearance of the target. In both cases, the first in the series of discrete prolate spheriodal sequences were used to window the data, which provided optimal frequency localization for each finite temporal window (Slepian 1983). This provided a frequency bandwidth of $\pm$ 0.25 and $\pm$ 5 Hz for the simulated and real data, respectively. We also investigated the results using the Fisher-transformed and bias-corrected z scores of coherence as described in Bokil et al. (2007) and found no differences in the pattern of results.

RESULTS

Basic model. Figure 2*C* shows the resulting coherence between simulated very low impedance electrodes and microelectrodes based on the basic model (Fig. 1, *A* and *B*). The simulated very low impedance electrodes had higher coherence than the simulated microelectrodes using both simulated (*left*) and real (*right*) LFP traces.

The basic result of Fig. 2*C* assumes a balance of subregion space corresponding to high and low distant coherence activity. If, on the other hand, a location is completely composed of a single subregion, a trivial consequence of the model is that the high and low impedance electrodes will record the same values. To further elucidate the entire relationship of these results to the spatial inhomogeneity of the underlying voltage coherence profile, we manipulated the high distant coherence fraction of the basic model (see MATERIALS AND METHODS) across a range of values (Fig. 3). As expected, when this fraction is near the limits of 0 and 1, smaller differences between the electrode types are observed. But at even modest departures from uniformity, considerable differences between the elec-

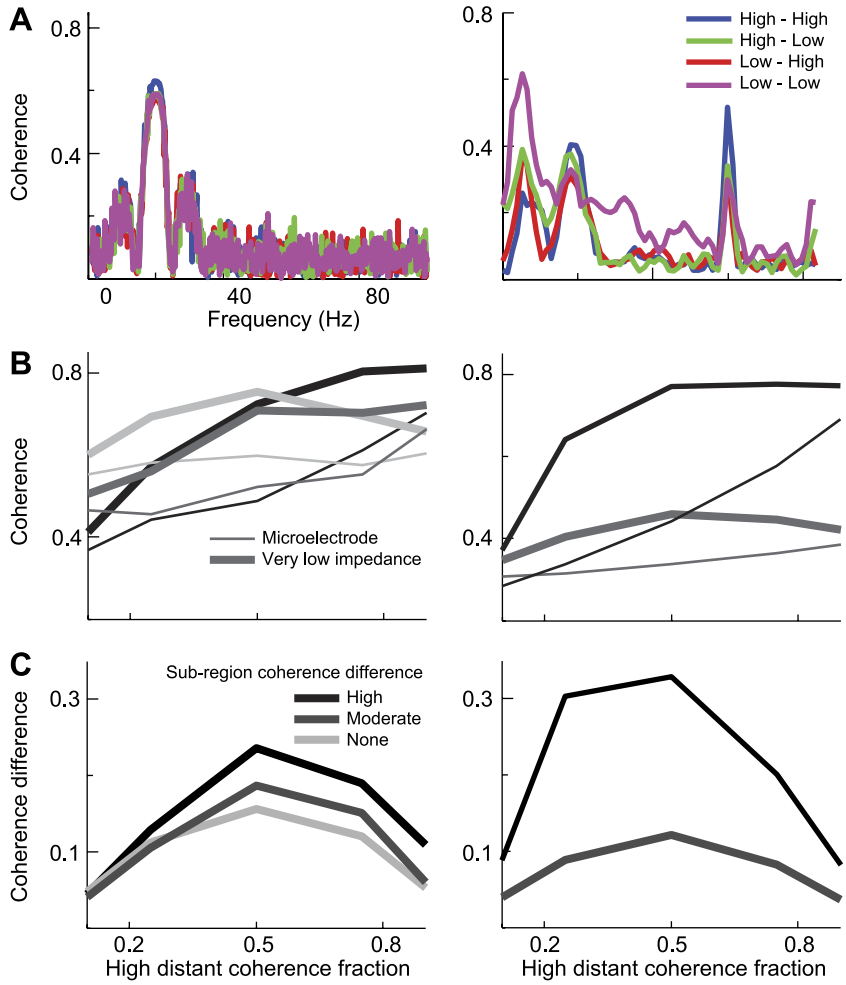

Fig. 4. Simulated coherence patterns of the basic model while varying the amount of coherence difference between subregions. *Left* panels correspond to results using simulated LFP traces, and *right* panels correspond to results using real LFP traces. *A*: direct intersubregion coherence across 2 locations as labeled for the 4 subregion combinations. *Left* panel reflects an example session of the simulations with no coherence difference between the individual traces (corresponding results shown in light gray in *B* and *C*). *Right* panel reflects an example session of real LFP traces selected to have approximately equally moderate coherence. Conventions are the same as in Fig. 2*B*. *B*: average 20-Hz coherence while varying the subregion coherence difference and the high distant coherence fraction. Both panels show the very low impedance electrode (thick) and microelectrode (thin) average 20-Hz coherence across 500 simulated sessions. Results where the underlying traces had high, moderate, or no coherence differences are shown in black, dark gray, and light gray, respectively. The high coherence difference results are duplicated from Fig. 3*B* and are shown here for comparison. *C*: difference in coherence between simulated very low impedance electrodes and microelectrodes for the data in *B*. Plotting conventions are the same as in *B*.

trodes appear. These differences peak when the voltage coherence profile is farthest from uniform.

The results of Fig. 3 show that when there is a relatively large difference in distant coherence between two subregions, averaging across them serves to increase the distant coherence reported. To what extent does this still occur when the voltages in the subregions are distinct, but with smaller or no differences in distant coherence between them? To investigate this, we simulated additional sessions using both simulated and real LFP traces with smaller or no coherence differences between the pairs of traces (see MATERIALS AND METHODS). Figure 4 shows that the increase in coherence for low impedance electrodes remained relatively strong for these simulations. Moreover, the increase continues to peak at a high distant coherence fraction of 0.5. Thus the inhomogeneity of an underlying voltage profile, regardless of its overall distant coherence gradient, appears to be the key factor driving this effect. These results were also consistent across further simulations we performed at different overall levels of coherence while varying the coherence differences between the trace pairs (results not shown). This further indicates the generality and robustness of this effect.

LFP, ECoG, and EEG comparisons. Given the effect shown by the basic model, one might expect electrode size differences to play a role when comparing coherences between EEG, ECoG, and LFP data, which are typically recorded with electrodes of very different sizes. EEG electrodes are typically 5–10 mm in diameter (Nunez and Srinivasan 2006), and ECoG electrodes tend to be about 2–5 mm in diameter for human studies (e.g., Canolty et al. 2006) or smaller for animal studies (e.g., Sharott et al. 2006; Taylor et al. 2005), whereas the recording sites for LFP electrodes can have lengths on the order of tens of micrometers or even smaller (Yaeli et al. 2009).

However, it is important to first note that the very nature of the underlying voltages themselves differs between these different sources of data. Cortical surface voltages underlying ECoG data are thought to be more spatially spread than intracranial voltages underlying LFP data (Nunez and Srinivasan 2006, 2010). Scalp voltages underlying EEG data are in turn thought to be more spatially spread than cortical surface voltages underlying ECoG data (Nunez and Srinivasan 2006, 2010). Thus electrode sizes cannot be directly compared between the data types, because the important factor described in the theoretical model that can lead to an effect of electrode size on recordings is the size of the electrode in relation to the spatial variation of the underlying voltage being measured. For example, the electrode size-related coherence effect that might result from one particular size of electrode when recording potentials at the cortical surface would be different than what would occur for the same electrode recording potentials either within the brain or on

the scalp. However, within each data type one can directly compare more moderate electrode size differences.

To demonstrate these differences between the data types and investigate whether any effects of electrode size on coherence within any of the data types might be subtly visible across published studies, we performed a quantitative literature search of published coherence values. Coherence will depend on a number of factors, including frequency and behavioral state, among others, although the effects of such factors can be difficult to predict (Bullock et al. 1995). However, coherence shows a direct and consistent dependence on electrode separation for all three data types, resulting largely from the volume conduction of electrical signals. Thus it is important to consider the interelectrode distance when comparing coherence across studies, and in particular across data types. In Fig. 5, we have plotted available data in the literature for the coherence of different data types as a function of interelectrode distance, documenting the electrode size and signal types for each data series. When possible, we selected the highest frequency data available in each study. We have noted the behavioral state of the subjects in each study in the Fig. 5 legend.

The differing spatial spread of the voltages underlying each data type is immediately apparent in Fig. 5. Similar coherences tend to be found at increased interelectrode distances for ECoG data relative to LFP data, and for EEG data relative to both ECoG and LFP data. For EEG data, scalp voltages are spatially spread out enough that recordings have been previously shown to be independent of electrode size for all practical purposes (Nunez and Srinivasan 2006). For ECoG data, however, further inspection of Fig. 5 reveals that a modest trend may exist for larger electrodes to report higher coherence. Notably, this was investigated directly in one study (Wang et al. 2009), which found that 3-mm-diameter electrodes showed higher coherence at the same interelectrode distances than 1.5-mm-diameter electrodes recorded from simultaneously in the same patient. This agrees with the qualitative prediction of the basic model described above. For LFP data, there are insufficient published coherence results at multiple electrode distances to allow us to come to an empirically based conclusion of the presence or absence of a noticeable effect of electrode size on typical recordings of that data type.

Spatial sine wave model. We used the spatial sine wave version of our model (Fig. 6*A*) to quantify when and to what extent the effect of electrode size found in the basic model is expected to occur, and further, to test whether this agrees with the trends in the literature data shown in Fig. 5. Figure 6*B* shows the resulting coherence for any ratio of an electrode's recording site length to the wavelength of the underlying spatial sine wave of activity in the model. This ratio captures the amount that the voltage profile changes over the extent of a recording site, which is the key factor described by the physical model as leading to possible effects of electrode size on recorded voltages. Moreover, this ratio provides a "common currency" to compare expected electrode size-related effects between data types, even as the nature of the underlying neural signals indeed varies between them. As anticipated given the results from the basic model, coherence generally increases as this ratio increases. However, at both very low and very high values of this ratio, the coherence becomes asymptotic and is generally insensitive to the precise electrode size. The results quantify a range between values of about 0.8 to about 8 where the ratio is more sensitive to the particular electrode size.

Quantitative predictions can be made from the information in Fig. 6*B* by specifying one of the two variables in the ratio. For example, the corresponding wavelength of the highest spatial frequency present above noise levels in the human

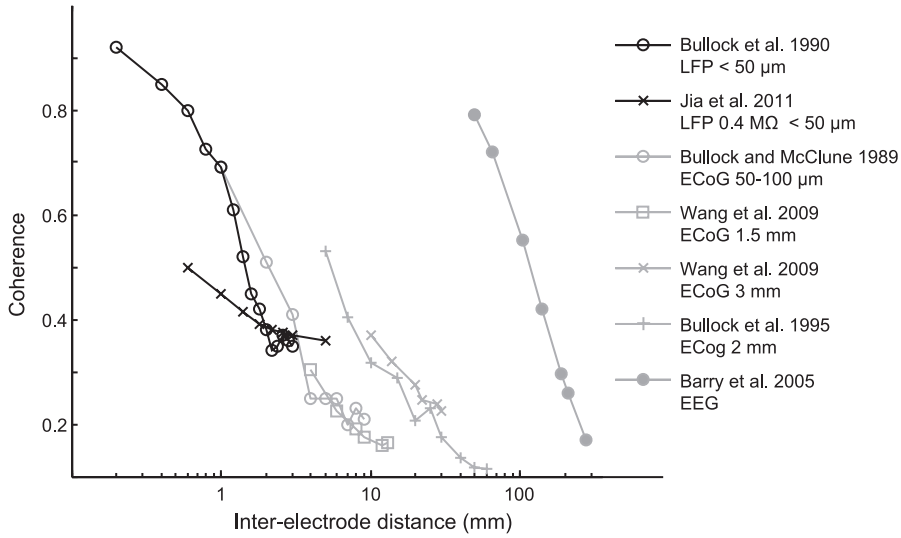

Fig. 5. Coherence against interelectrode distance data in the literature for LFP, electrocorticogram (ECoG), and electroencephalogram (EEG) data. The source reference is cited, and the data type and the approximate electrode diameter for each data series are shown. Bullock et al. (1990) data are from their Fig. 2*B*, 20–40 Hz, collected during slow-wave sleep and paradoxical sleep. We report the average across these two values. This study lists the electrode shank diameter to be 50 μm, suggesting the diameter across the uninsulated tip is at least smaller than this. Jia et al. (2011) data are from their Fig. 8*D*, 30–50 Hz, showing spontaneous activity with the subject under anesthesia. This study indicates the electrodes used had impedances of 0.4 MΩ. Given the geometrical constraints and the relation between impedance and surface area described in Yaeli et al. (2009), this likely suggests a tip size $<$50 μm. Bullock and McClune (1989) data are from their Fig. 4, *bottom* panel, 35–40 Hz, collected with the subject under light anesthesia. Wang et al. (2009) data are from their Fig. 2*B*, 60–120 Hz, collected with the subject awake and relaxed with eyes open. Bullock et al. (1995) data reflect averages of data shown in their Figs. 3, 4, and 5, corresponding to frequency ranges spanning from 20 to 80 Hz, collected during slow-wave sleep, alert, or sedated behavioral states. Barry et al. (2005) data are from the regression line in their Fig. 1, *top* panel, 1.5–25 Hz, collected with the subject in an awake resting state with eyes closed.

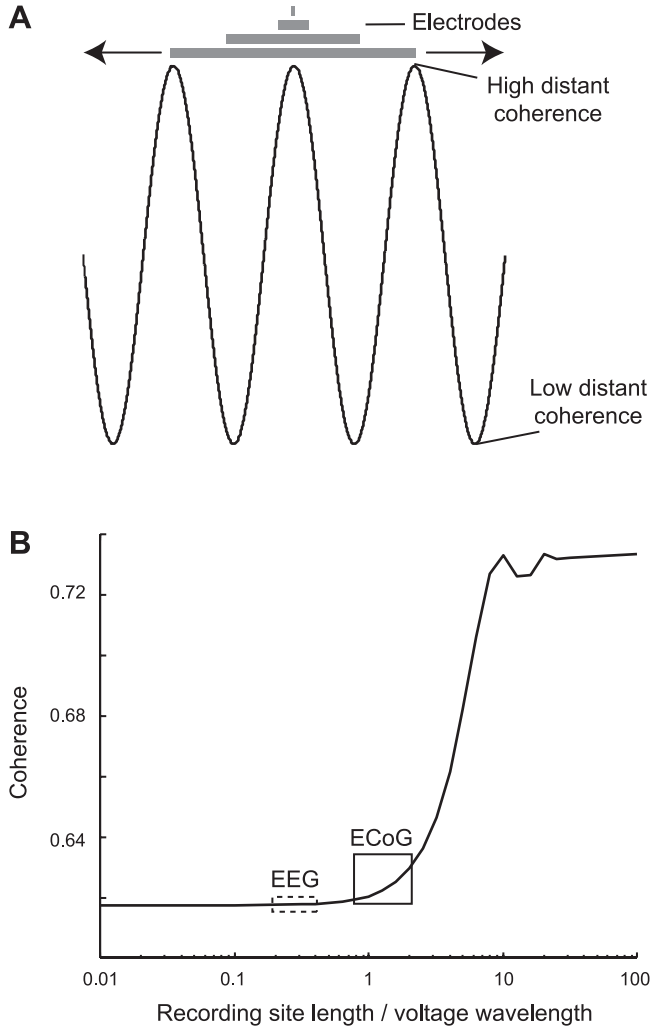

Fig. 6. Spatial sine wave model and results. *A*: model illustration. In this version of the model, the amount of distant coherence at each point in space is varied continuously following a sine wave. Different sizes of electrode recording sites are modeled to average the underlying activity along their lengths with a randomly selected initial phase for each simulated session. *B*: simulated coherence plotted against the ratio of electrode recording site length to the wavelength of the sinusoidal voltage profile. The average 20-Hz coherence across sessions using simulated data is shown. The putative ranges corresponding to typical EEG and ECoG electrodes at the corresponding highest spatial frequency of the voltage underlying each data type are indicated. For LFP recordings, this spatial frequency is presently not clearly known.

cortical surface potential has been estimated to be 2.5 mm per cycle (Freeman et al. 2000). For this spatial frequency, this ratio for typical ECoG electrodes would range between 0.8 and 2.0, as indicated in Fig. 6*B*. Modest effects of electrode size on coherence are indeed expected within this range, which is consistent with Wang et al. (2009) and the other ECoG studies shown in Fig. 5. In contrast, the corresponding wavelength of the highest spatial frequency present above noise levels in the human scalp potential has been estimated to be 2.5 cm per cycle (Freeman et al. 2003). For this spatial frequency, this ratio for typical EEG electrodes would range between 0.2 and 0.4, as indicated in Fig. 6*B*. No appreciable effects of electrode size are expected within this range, which confirms previous evidence that EEG data is independent of electrode size for the electrodes typically used to record it. For LFP data, the highest spatial frequency present above noise level within the brain has not yet directly been shown. However, although it is not a simple step to convert the estimates of the point spread function from Katzner et al. (2009) and Xing et al. (2009) into a maximum spatial frequency, a wavelength on the order of 250 μm per cycle might provide a reasonable educated guess. At this voltage profile wavelength, it seems reasonable that a 200-μm-diameter electrode (with a corresponding ratio of 0.8) might show subtle increases in coherence in some studies (Kay and Lazarra 2010) but not others (Bullock et al. 1989). This would also suggest, however, that differences among the smaller sizes of microelectrodes typically used during depth recordings would not occur. More evidence of this spatial frequency limit in intracranial voltage is needed, however, to draw firmer conclusions about the model's prediction.

DISCUSSION

We have developed and tested a simple physical model for LFP recordings of electrodes with large differences in recording site sizes. The model predicts that low impedance electrodes tend to report higher coherence than higher impedance microelectrodes. However, intrinsic to the model is that voltages must vary on a spatial scale smaller than the size of the larger electrode recording site for the electrode size to make a difference. Moreover, this difference between electrode sizes continuously increases as the voltage profile over the length of the electrode's recording site is increasingly inhomogeneous. This effect is robust with respect to the strength of the coherence gradient along the spatial voltage profile. We compared previously published reports in the literature for the coherence of LFP, ECoG, and EEG data and found evidence for a modest effect of electrode size in ECoG data, but not in EEG or LFP data. We further developed the model to quantify at what electrode sizes relative to a given voltage profile spatial frequency the electrode size is expected to impact recorded coherence. Combining this with estimates in the literature for the spatial frequencies present in all these data types confirms the suggestions of the literature data.

As the model points out, the suggestion that a pair of lower impedance electrodes favors distantly coherent activity relies on the spatial voltage profiles at the two recording locations. For the extreme example of spatially uniform voltages, the model trivially shows that there would be no expected effect of recording site size. However, as the voltage profiles increasingly depart from uniform, both the basic model and the spatial sine wave model confirm that the electrode size effect continuously increases. In the basic model, this can be observed as the high distant coherence fraction changes (Figs. 3 and 4). In the spatial sine wave model, this can be observed as the coherence increases continuously as the number of voltage profile cycles along a recording site's length increases (Fig. 6), excluding the plateaus observed for relatively very small or very large electrodes. The additional simulations varying the coherence gradient (Fig. 4) further show that this effect is general to any voltage gradient, regardless of the amount that the distant coherence changes along it. It should be emphasized that though there were small or no coherence differences between the combinations of trace pairs used for these additional simulations, the individual traces were still distinct and sufficiently independent of each other, which is required for the effect to occur.

As we mentioned, the results of the spatial sine wave version of the model shown in Fig. 6 can be used to estimate effects for LFP, ECoG, or EEG data. The precision of any practical implication of the model, however, is limited by the accuracy of the knowledge of the spatial frequencies present in the underlying voltages. For LFPs, the scale of this spatial variation has yet to be sufficiently quantified. Still, the estimates of Katzner et al. (2009) and Xing et al. (2009) do clearly suggest that LFP voltages will not appreciably vary on a scale of tens of micrometers, which are the lengths of electrode recording sites in typical use by neurophysiologists (Yaeli, et al. 2009). Thus the effects of microelectrode sizes for recording LFPs should be negligible, as we have argued (Nelson and Pouget 2010).

For ECoG data, further empirical evidence may be needed to corroborate the putative effect that we have shown in literature data and our simulations. This evidence would be useful in the form of either further direct tests similar to the study of Wang et al. (2009) or corroboration of the estimates of Freeman et al. (2000) of the spatial frequencies present in cortical surface potentials. If it holds true, the effect for ECoG data would not suggest per se that data from larger electrodes is faulty. Rather, it would just be an effect that must be kept in mind when interpreting that data, particularly when considering coherence.

The model we present implies that once the electrode size is small enough relative to the spatial variation of the underlying voltages being measured, recorded data should be independent of electrode size. This together with well-understood sampling theory dictates that using such sufficiently small electrodes with interelectrode spacing that is small enough to avoid spatial aliasing of the signal guarantees the ability to recover all of the information present in the underlying voltages. Thus it may be advisable to attempt to accomplish this during EEG, ECOG, or LFP electrode array design, although it is conceivable that some trade-offs and limitations surrounding this may exist for some applications. Still, knowledge of the physical model of electrode recordings and the nature of the underlying signals one is trying to record should prove helpful for the choice and design of arrays for any application.

It should also be noted that multiple spatial frequencies are present in LFP, ECoG, and EEG data. Our results show that the effect of electrode size, to the extent that it exists at all for a given data type, should be increasingly larger for the higher spatial frequency signals present. The ranges shown in Fig. 6 for EEG and ECoG data correspond to the most affected spatial frequencies for these data types. Each data type also includes contributions from lower spatial frequency signals as well, which would correspond to regions to the left of these indicated ranges on the plot.

The model we present also suggests that the variance of coherence across sessions for different electrode sizes would be an interesting quantity to investigate empirically, with the prediction that this should be higher for smaller electrodes whenever the coherence is dependent on electrode size.

The model that we present is an intentionally simple model targeted at the electrodes themselves and exploring the theoretical physical nature of how and under what circumstances the sizes of their recording sites might affect their performance. Biological sources of signals could certainly be modeled, but the implications resulting from this would be tangential to our focus on electrodes and would come at a cost of undesirable added complexity. The basic model we tested applies the most extreme version of a spatial voltage gradient, essentially a step function, to demonstrate whether or not the effect could be a possibility for less extreme, more realistic profiles. This does not reflect a presumption that voltages in the brain would actually change as a step function between boundaries. Beyond this, the spatial sine wave model allows us to generalize to the expected effect for any spatial frequency present in the voltage profile. More complicated profiles could of course be modeled, but as Fourier analysis dictates, these would be identical to a summation of spatial sinusoids of different frequencies.

Existing studies have modeled electrode size under different contexts than what we have done here. Ollikainen et al. (2000) considered the electrical shunting effect of covering the scalp with conductive EEG electrodes. A notable pair of studies (Lempka et al. 2011; Moffitt and McIntyre 2005) modeled the effect of electrode recording site size on recording spiking activity within the brain by using a more complex finite element model with realistic biological sources of both the signals being measured and the noise occluding it. Recording site sizes affect their model by changing the conductivity on the particular locations of an electrode between the much lower value for that of recording sites and the much higher value for that of the insulated shank. Thus the model they present does not directly look at the effects of simple spatial averaging of potentials as the model we present does. A further inspection of their model might reveal a near equivalence to that of the simple model we present here. However, it is not immediately clear that this is the case. Notably, in their description of their model or their results, the authors never explicitly mention this property of spatial averaging, which is inherent to the physical model of electrode recordings espoused by Robinson (1968). Further inspection of this in the model they present could be of theoretical interest. Interestingly, the model they present produces results for spiking activity amplitude that are similar to what we show here for LFP, ECoG, and EEG coherence. Specifically, they suggest that spike recording is fairly independent of recording site size over the range of contact sizes typically employed by neurophysiologists [177–1,250 μm^2, the tungsten microelectrode equivalent of about 2.4- to 0.5-MΩ impedances (Yaeli et al. 2009)], but they did find decreased amplitudes for a very large electrode that they simulated [10,000 μm^2, the tungsten microelectrode equivalent of at least $<$0.1-MΩ impedance (Yaeli et al. 2009)].

In contrast, the model we present is macroscopic and considerably simple. We believe this is the appropriate level of complication for the aim of this study, which was to provide a simple intuitive model for members of the field to understand and apply. This is in contrast to more complicated models that may be treated too often as a "black box" by many readers, rather than engendering an intuitive understanding of their underlying function.

We believe more adherence to and understanding of the physical nature of electrode recordings in the field and in the literature will aid the discussion of the putative effects of recording site shape and size on recorded potentials. Too many previous claims in the literature that these properties are important to account for while interpreting LFP data (Berens et al. 2008; Kay and Lazarra 2010; Pesaran 2009) do not appear to adhere to any theoretical basis or provide any explanations as to precisely how or why effects of these properties would

come about. The simple model we explore in our simulations provides a more solid theoretical basis on which to judge these claims. The results for LFP data indicate, to the contrary, that these properties likely do not have a substantial effect for the electrodes typically employed by neurophysiologists. Data comparing microelectrodes of different impedances within this range of typical use will clearly be important to draw firmer conclusions.

ACKNOWLEDGMENTS

We thank Jeff Schall for graciously sharing data collected in his laboratory. M. Nelson was supported by the Programme de bourses d'excellence Eiffel.

DISCLOSURES

No conflicts of interest, financial or otherwise, are declared by the author(s).

AUTHOR CONTRIBUTIONS

Author contributions: M.J.N. and P.P. conception and design of research; M.J.N. performed experiments; M.J.N. analyzed data; M.J.N. and P.P. interpreted results of experiments; M.J.N. prepared figures; M.J.N. drafted manuscript; M.J.N. edited and revised manuscript; M.J.N. and P.P. approved final version of manuscript.

REFERENCES

Barry RJ, Clarke AR, McCarthy R, Selikowitz M. Adjusting EEG coherence for inter-electrode distance effects: an exploration in normal children. *Int J Psycholphysiol* 55: 313–321, 2005.

Bedard C, Rodrigues S, Roy N, Contreras D, Destexhe A. Evidence for frequency-dependent extracellular impedance from the transfer function between extracellular and intracellular potentials. *J Comput Neurosci* 29: 405–421, 2010.

Berens P, Keliris GA, Ecker AS, Logothetis NK, Tolias AS. Feature selectivity of the gamma-band of the local field potential in primate primary visual cortex. *Front Neurosci* 2: 199–207, 2008.

Bokil H, Purpura K, Schoffelen JM, Thomson D, Mitra P. Comparing spectra and coherences for groups of unequal size. *J Neurosci Meth* 159: 337–345, 2007.

Bullock TH, Buzsaki G, McClune MC. Coherence of compound field potentials reveals discontinuities in the CA1-subiculum of the hippocampus in freely-moving rats. *Neuroscience* 38: 609–619, 1990.

Bullock TH, McClune MC. Lateral coherence of the electrocorticogram: a new measure of brain synchrony. *Electroencephalogr Clin Neurophysiol* 73: 479–498, 1989.

Bullock TH, McClune MC, Achimowicz JZ, Iragui-Madoz VJ, Duckrow RB, Spencer SS. EEG coherence has structure in eth millimeter domain: subdural and hippocampal recordings from epileptic patients. *Electroencephalogr Clin Neurophysiol* 96: 161–177, 1995.

Canolty RT, Edwards E, Dalal SS, Soltani M, Nagrajan SS, Kirsch HE, Berger MS, Barbaro NM, Knight RT. High gamma power is phase-locked to theta oscillations in human neocortex. *Science* 313: 1626–1628, 2006.

Freeman WJ, Holmes MD, Burke BC, Vanhatalo S. Spatial spectra of scalp EEG and EMG from awake humans. *Clin Neurophysiol* 114: 1053–1068, 2003.

Freeman WJ, Rogers LJ, Holmes MD, Silbergeld DL. Spatial spectral analysis of human electrocorticograms including the alpha and gamma bands. *J Neurosci Meth* 95: 111–121, 2000.

Jarvis MR, Mitra PP. Sampling properties of the spectrum and coherency of sequences of action potentials. *Neural Comput* 13: 717–749, 2001.

Jia X, Smith MA, Kohn A. Stimulus selectivity and spatial coherence of gamma components of the local field potential. *J Neurosci* 31: 9390–9403, 2011.

Katzner S, Nauhaus I, Benucci A, Bonin V, Ringach DL, Carandini M. Local origin of field potentials in visual cortex. *Neuron* 61: 35–41, 2009.

Kay LM, Lazzara P. How global are olfactory bulb oscillations? *J Neurophysiol* 104: 1768–1773, 2010.

Lemon R. *Methods for Neuronal Recording in Conscious Animals.* Chichester, NY: Wiley-Interscience, 1995, p. 74–75.

Lempka SF, Johnson MD, Moffitt MA, Otto KJ, Kipke DR, McIntyre CC. Theoretical analysis of intracortical microelectrode recordings. *J Neural Eng* 8: 045006, 2011.

Logothetis NK, Kayser C, Oeltermann A. In vivo measurement of cortical impedance spectrum in monkeys: implications for signal propagation. *Neuron* 55: 809–823, 2007.

Moffitt MA, McIntyre CC. Model-based analysis of cortical recording with silicon microelectrodes. *Clin Neurophysiol* 116: 2240–2250, 2005.

Murthy A, Thompson KG, Schall JD. Dynamic dissociation of visual selection from saccade programming in frontal eye field. *J Neurophysiol* 86: 2634–2637, 2001.

Nelson MJ, Pouget P. Do electrode properties create a problem in interpreting local field potential recordings? *J Neurophysiol* 103: 2315–2317, 2010.

Nelson MJ, Pouget P, Nilsen EA, Patten CD, Schall JD. Review of signal distortion through metal microelectrode recording circuits and filters. *J Neurosci Methods* 169: 141–157, 2008.

Nunez PL, Srinivasan R. *Electric Fields of the Brain: The Neurophysics of EEG* **(2nd ed.)**. New York: Oxford University Press, 2006.

Nunez PL, Srinivasan R. Scale and frequency chauvinism in brain dynamics: too much emphasis on gamma band oscillations. *Brain Struct Funct* 215: 67–71, 2010.

Ollikainen JO, Vauhkonen M, Karjalainen PA, Kaipio JP. Effects of electrode properties on EEG measurements and a related inverse problem. *Med Eng Phys* 22: 535–545, 2000.

Pesaran B. Uncovering the mysterious origins of local field potentials. *Neuron* 61: 1–2, 2009.

Robinson DA. The electrical properties of metal microelectrodes. *Proc IEEE* 56: 1065–1071, 1968.

Sharott A, Magill PJ, Bolam JP, Brown P. Directional analysis of coherent oscillatory field potentials in the cerebral cortex and basal ganglia of the rat. *J Physiol* 562: 951–963, 2005.

Slepian D. Some comments on Fourier analysis, uncertainty and modeling. *SIAM Rev Soc Ind Appl Math* 25: 379–393, 1983.

Taylor K, Mandon S, Freiwald WA, Kreiter AK. Coherent oscillatory activity in monkey area V4 predicts successful allocation of attention. *Cereb Cortex* 15: 1424–1437, 2005.

Tielen AM, Giesen C, Mollevanger W. Some mechanical and electrical characteristics of metal microelectrodes. *Inst Med Phys TNO Rep* 2.3.65/1 MEI, 1971.

Wang W, Degenhart AD, Collinger JL, Vinjamuri R, Sudre GP, Adelson PD, Holder DL, Leuthardt EC, Moran DW, Boninger ML, Schwartz AB, Crammond DJ, Tyler-Kabara EC, Weber DJ. Human motor cortical activity recorded with micro-ECoG electrodes during individual finger movements. *Conf Proc IEEE Eng Med Biol Soc* 2009: 586–589, 2009.

Xing D, Yeh CI, Shapley RM. Spatial spread of the local field potential and its laminar variation in visual cortex. *J Neurosci* 29: 11540–11549, 2009.

Yaeli S, Binyamin E, Shoham S. Form-function relations in cone-tipped stimulating microelectrodes. *Front Neuroeng* 2: 13, 2009.